Electric Power Systems Research 174 (2019) 105871

Contents lists available at ScienceDirect

Electric Power Systems Research

journal homepage: www.elsevier.com/locate/epsr

Grounding systems under lightning surges with soil ionization for high voltage substations by using two layer capacitors (TLC) model

Samy M. Ghania

Benha University, Cairo, Egypt

ARTICLE INFO

Keywords:
Index terms- grounding systems modeling
Soil ionization
Two layer capacitors (TLC)
Time domain analysis with FDTD
lightning surges

ABSTRACT

The grounding system behavior in the time domain for the high voltage substations is the key-parameter to ensure the system reliability during transient conditions. Many approaches are used to investigate the behavior of the grounding systems subjected to the lightning surges. These approaches aim to simplify the grounding systems by equivalent lumped circuit-parameters (RLC) or by using the electromagnetic field theory. The soil ionization phenomenon can effectively reduce the grounding electrode resistance because of changing the electrode equivalent radius located in the soils. Yet, most of these approaches have their relative assumptions with merits and demerits. The current work introduces a proposed model based on a developed grounding unit cell using the Two Layer Capacitors (TLC). The proposed cell is implemented as a unit cell to simulate the performance of the grounding system under lightning strikes with considering the soil ionization effects. Different developed models of the grounding-cells are used to simulate the behavior of the grounding system including the soil ionization process. Finite Difference Time Domain FDTD scheme is used to calculate the electromagnetic fields inside the different proposed unit cells during lightning surges. The application of the grounding unit cell is extended to be implemented for a typical high voltage substation of 500/220 kV. The grounding unit cells are presented as T neighboring sections to evaluate the overlapping between the different elementary electrodes and conductors of the complex grounding systems over the whole area of the substation. The circuit-model of the grounding unit cell is developed using EMTP-RV/MATLAB. Finally, the obtained results are compared with the similar results found in the literature with good consistency.

1. Introduction

Grounding system inside electrical power substations plays a vital role in the protection and reliability studies since the early days of power systems installation. Grounding system must provide a safe and effective diverted path for the high surges to earth [1–3]. The grounding systems have to sufficiently secure low impedance and high current-carrying capacity to prevent grounding potential rise (GPR) that may result in any occupational hazards to the connected equipment and to any person as well. Performance of the grounding systems under normal and fault conditions is properly explained and demonstrated in Refs. [4–7]. The transient performance of grounding systems under lightning surges is quite different [8]. Transient response of the grounding systems under lightning surges is nonlinear because of the prospective of soil ionization [9]. However, the soil ionization and the nonlinearity of the grounding systems effects have not been plainly tackled. Most likely, because of these difficulties, when the grounding system is analyzed under lightning surges, the nonlinear ionization phenomenon is often ignored [10,11]. The Finite Difference Time Domain (FDTD) is a simple and efficient method for solving Maxwell equations for a wide variety of problems. The transient and steady state performance of the grounding systems are evaluated using the FDTD [12,13]. A Model of a large grounding system using FDTD calculation has been developed to calculate the transient impedance of the grounding system accurately. The FDTD scheme provides no more needs for excessive computational resources [14,15]. The soil ionization process can occur when earth electrodes are injected by intensive pulse transient currents such that yield from lightning surges. The soil ionization begins when the electrical field on the grounding electrodes surface overcomes the soil dielectric strength. The soil ionization problem is originally expressed as a nonlinear and variable time function [16]. To avoid the needs for formulating some hypotheses regarding the shape of the soil ionization regions of the grounding system under lightning surges, a numerical solution of Maxwell equations using FDTD is developed in Ref. [17]. Different approaches are developed to tackle the study of the soil resistivity during the ionization and subsequent de-ionization process. Nevertheless, the variable soil conductivity hypotheses found in the literature still needs to be enforced to properly

E-mail addresses: samy_ghania@yahoo.com, samy.ghaniah@Feng.bu.edu.eg.

https://doi.org/10.1016/j.epsr.2019.105871
Received 4 December 2017; Received in revised form 20 December 2018; Accepted 8 May 2019
Available online 23 May 2019
0378-7796/

investigate the soil ionization around the grounding electrodes/conductors due to lightning surges [18–20]. Ionization phenomenon is a process that locally appears in the regions where a current with intensive density is discharged into the soil. Consequently, paths with conductive plasma can be established inside the ionized zone [21]. Most likely, the soil is often considered to be homogeneous and isotropic. Hence, ionization is assumed to be uniform in the soil around the electrodes. There are some hypotheses about the shape of the ionized zone [22]. The soil electrical conductivity is a complicated problem especially with the presence of many variable parameters. The main dominant parameters depend on the size and the distribution of the non-conductive particles besides to the amount of water and the amount of salt dissolved in the water. Therefore, the air gaps within the soil have highly irregular shapes especially if the surrounding pieces have sharp edges [23]. The main objective of the current work is investigating the transient performance of the grounding systems under surges by developing a new model with different developed grounding unit-cells as lamped parameters. This new model presents the effects of the soil ionization on the transient grounding potential rise GPR in time domain. The new proposed numerical model of the soil ionization phenomena is developed based on a grounding unit cell using the Two Layer Capacitors (TLC). The developed grounding unit cell is used to simulate the earthing electrodes and conductors during lightning surges. Different TLCs unit-cells are modelled to be implemented for simulating the whole grounding grids with consideration of the ionization phenomena. The FDTD algorithm is used to calculate the electromagnetic fields distribution during the lightning surges over the grounding grid-unit. With extending the implementation of the grounding unit cell, the grounding system is simulated inside a typical high voltage substation of 500/220 kV. The mutual and overlapping impedances between the unit cells are computed to present the effects of the different elementary electrodes and conductors of the complex grounding systems over the whole area of the substation. The circuit-model of the grounding unit cell and the whole system are developed using EMTP-RV/MATLAB. Finally, validation of the proposed model is performed by comparing the simulation results with simulated and experimental data found in literature work.

2. Modelling of the soil ionization

2.1. Soil microstructure and ionization

Microstructure of the soil shows that it is a mixture of fragmented mineral materials, gases and organic matters. Air voids are existing among the soil particles [24]. These voids are with nonuniform sizes and distributions as well. Soil ionization process is initiated because of the breakdown inside the air voids enclosed among the soil particles. This breakdown is established when grounding electrodes and conductors are subjected to impulse currents such as that caused by lightning surges. Some models are developed based on the numerical solution of Maxwell's equations and on the space-time variable soil conductivity approach using Finite Difference Time Domain FDTD [25,26]. The soil ionization region is modeled as Two Layer Capacitors (TLC) network. This approach integrated with Finite Difference Time Domain are adopted to develop the grounding grid unit-cell of the proposed current model to simulate the soil ionization zone. The developed equivalent circuit contains key components including soil and arc resistances and soil capacitances are shown in Fig. 1. Two Layer Capacitors (TLC) is used to model the different permittivity values of the soil particles and air voids. It is assumed that all the soil particles have the same permittivity/conductivity value and all the air voids do as well. In addition, the dimensions of both soil particles and air voids are uniform as shown in Fig. 1. Because of lower soil particles resistance relative to air voids resistance, the surge current flows through the soil particles during no ionization (Fig. 1a). Hence, the series soil resistance is represented by equivalent R_{soil}. The equivalent capacitances of the

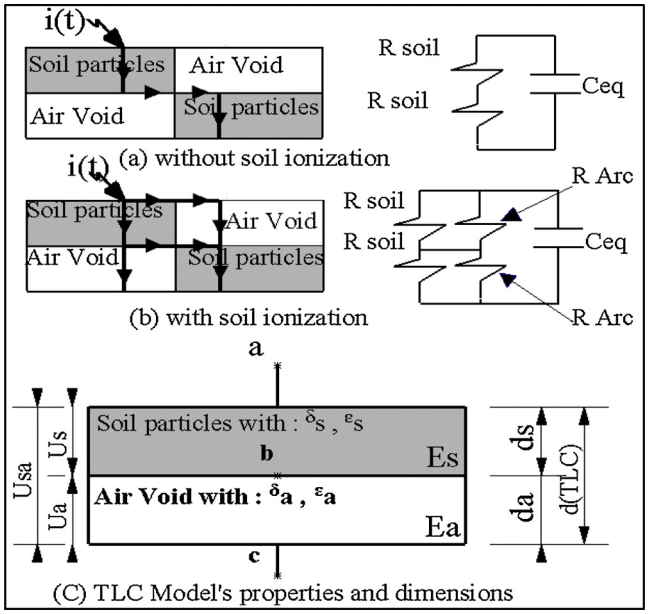

Fig. 1. Proposed model of the soil with and without ionization process and the TLC properties and dimensions [24].

soil particles and air voids are represented by C_{eq}. The soil C_{soil}, and air voids C_{air} can be determined according to $C = \varepsilon A/d$, where ε is the permittivity, d is the length of the soil particle and air void, and $A = d^2$ and d is determined by using the method proposed in Ref. [27]. The soil ionization means breakdown that occurs inside the air voids enclosed among the soil particles when grounding electrodes are subjected to intensive impulse stresses. This occurs as the electric field of the air voids exceeds a critical limit which is the soil electric field value E_c. The major component of the surge current flows through the ionized air voids (Arcs). Consequently, during ionization process, the arc capacitance is negligible and C_{eq} is only for the soil particles. All above described parameters will be further developed into a TLC network. Table 1 presents the range of the different soil particles and its sized based on British soil classification system [28].

2.2. Determination of the TLC parameters

The Two Layer Capacitors (TLC) parameter values for soil ionization can be physically determined based on the type of the soil. The type of soil is determined based on the average soil resistivity and its resistance as explained in IEEE Std. [29]. Fig. 1 (C) shows the schematic of the typical proposed TLC dimensions and different parameters. The parameters of the d_s and d_a are the lengths of the soil particles and air voids, respectively. The value of d_a is proportionally related to d_s [30,31]. The

Table 1
Soil particle sizes based on the British soil classification system.

Very coarse soils	Boulders		> 200 mm
	Cobbles		60–200 mm
Coarse soils	Gravel	Coarse	20–60 mm
		Medium	6–20 mm
		Fine	2–6 mm
	Sand	Coarse	0.6–2.0 mm
		Medium	0.2–0.6 mm
		Fine	0.06–0.2 mm
Fine soils	Silt	Coarse	0.02–0.06 mm
		Medium	0.006–0.02 mm
		Fine	0.002–0.006 mm
	Clay		< 0.002 mm

Table 2
Parameter values for developing TLC model.

Parameters	Proposed model parameters
Soil type, IEEE std. [29]	Sand Fine
Soil resistivity, ρ (Ω m)	100
Soil relative permittivity, ε_r	10
Electrode length, l (m)	3
Electrode radius, r (mm)	13
Current"s amplitude I_m (kA)	100
Critical electric field Ec (kV/m)	370
Current"s T_f/T_h (μs/μs)	(1.2/50)
ds, (mm)	0.2
da, (mm)	0.001
Usa, (V)	1.1
σ_a (Air void conductivity (S/m))	$1 \times 10^{(-17)}$
σ_s (soil particle conductivity (S/m))	$3 \times 10^{(-17)}$

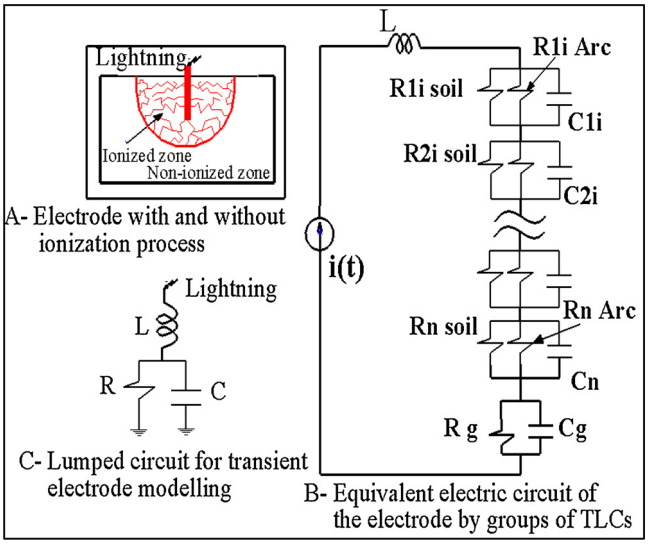

Fig. 2. Electrical equivalent circuit of the grounding electrode with multi-TLCs under impulse condition with and without ionization.

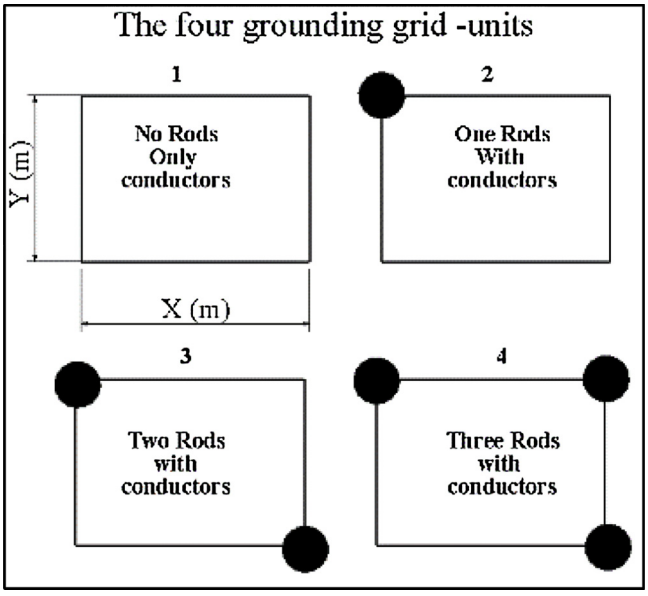

Fig. 3. The proposed four grounding grid-units. (A) The substation schematic layout. (B) Typical grounding grid.

voltage across the TLC is U_{sa}. Because of the different values of the permittivity (ε) and the conductivity (σ) of the soil particles and air voids, the voltages across the soil particles U_s and U_a are different. Consequently, the electric fields E_s and E_a are different as well. It is assumed that a surge current i(t) is applied at point a. The surge voltages at points a and b w.r.t point c are $U_a(t)$ and $U_s(t)$. The whole applied surge voltage is $U_{sa}(t)$ potentially divided over the soil particle (U_s (t)) and the air void (U_a (t)) as presented in Fig. 1. The corresponding electric fields as a function of time can be computed using Eqs. 1 and 2. The electric fields are varied inside both soil particle and in the air void. Hence a time lag to breakdown t_i inside air void after applying voltage U_{sa} with time t_u is initiated. The time t_i is the required time for the air breakdown under surge stress that causes ionization process inside air voids. This will lead to the total time that causes the breakdown inside the air voids as $T_{br} = t_u + t_i$. It is assumed that $\in_s \neq \in_a$ and $\sigma_s = 3^* \sigma_a$ (the typical values are presented in Table 2). The electric field of the soil particle and air void will be given by Eqs. 1 and 2:

$$E_s(t) = \frac{\sigma_a}{\sigma_s + \sigma_a}.\frac{U_{sa}}{d_s} - \left(\frac{\sigma_a}{\sigma_s + \sigma_a} - \frac{d_s \in_a}{d_s \in_a + d_a \in_s}\right)\frac{U_{sa}}{d_s} e^{-\frac{t}{\tau}} \quad (1)$$

$$E_a(t) = \frac{\sigma_s}{\sigma_s + \sigma_a}.\frac{U_{sa}}{d_a} - \left(\frac{\sigma_a}{\sigma_s + \sigma_a} - \frac{d_a \in_s}{d_s \in_a + d_a \in_s}\right)\frac{U_{sa}}{d_a} e^{-\frac{t}{\tau}} \quad (2)$$

where the time constant is given by

$$\tau = \frac{d_a \sigma_s + d_s \sigma_a}{d_a \in_s + d_s \in_a} \quad (3)$$

The approximate length of the ionization zone x can be determined as the total number (n) of the consecutive and ionized TLCs as given in Eqs. 4 and 5. The breakdown in each TLC is assumed to occur consecutively from the first to the last TLC. The breakdown of the last TLC occurs when the injected current reaches its maximum. This will be indicated as the maximum soil ionization length x_{max}. Once the soil ionization length is increased, the grounding resistance will be highly affected. The effect of ionization on grounding resistance will be investigated by multi-forms of the electrical equivalent network.

$$X = \sum_{i=1}^{n} d_{TLC} \quad (4)$$

$$X_{\max} = n^* d_{TLC} \quad (5)$$

The maximum length of the ionization zone $\boldsymbol{x}_{max}$ is adopted for the horizontal and vertical electrodes as given by Eqs. 6 and 7, respectively. The equivalent grounding resistance for the horizontal conductors and the vertical electrodes can be presented as given in Eqs. 9 and 10, respectively. The frequency-dependence of soil electrical conductivity and permittivity in its response to lightning currents shows a significant reduction of the amplitude values of the transient voltages and impulse impedance. Moreover, it increases the expected effective length and radius of the grounding electrodes. These effects will significantly change the grounding electrode parameters as included in Eqs. 6–10. Accordingly, the soil parameters and the different dimensions of the electrode and burial depth underneath the ground surface should be considered as an effective parameter of the soil ionization.

$$X_{\max} = \frac{2l^2}{de^{2\left(\frac{k\pi lR}{\rho}+1\right)}} - a \quad (6)$$

And for the vertical electrode

$$X_{\max} = \frac{4l}{e^{\left(\frac{k\pi lR}{\rho}+1\right)}} - a \quad (7)$$

$$k = \frac{1}{\sqrt{1 + \frac{2\pi l_m R^2}{E_c \rho}}} \quad (8)$$

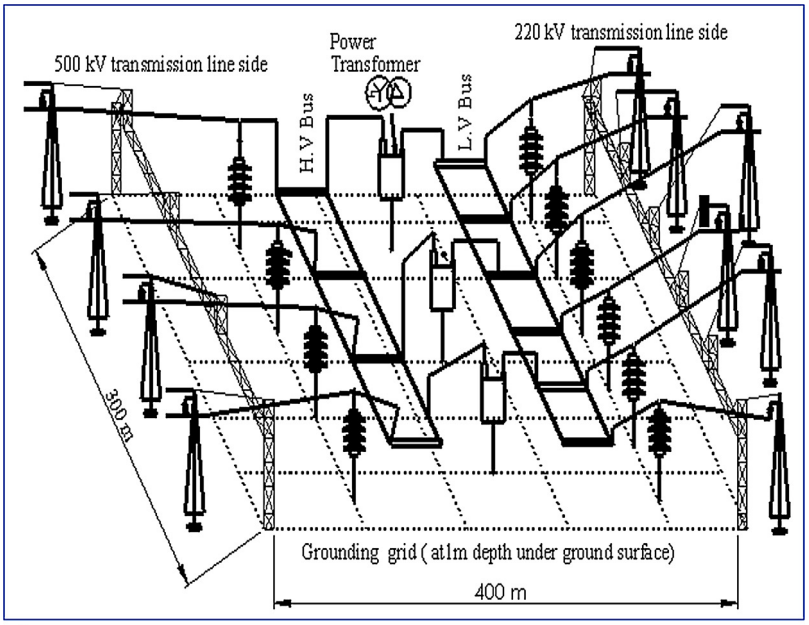

Fig. 4. The typical grounding grid area and the substation schematic layout (not to scale).

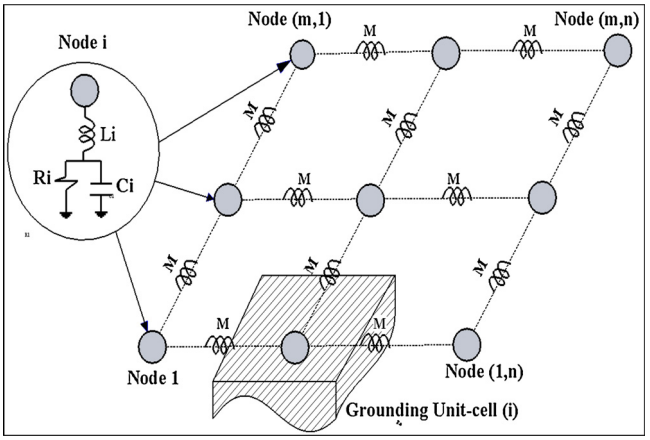

Fig. 5. Electrical equivalent circuit for grounding electrode and grounding grid with the mutual between each unit-cell.

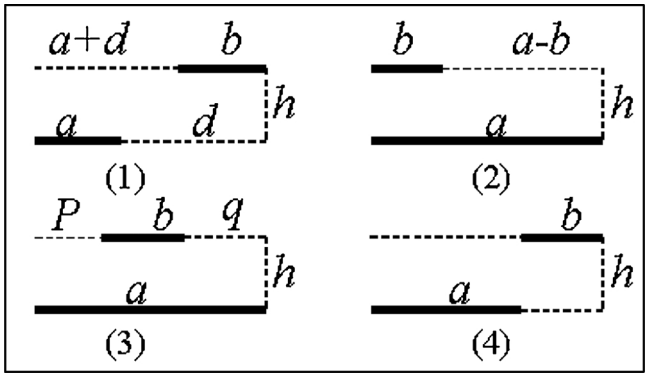

Fig. 6. Different parallel conductor's arrangements. (A) Flow chart of the developed system. (B) Screenshot of a part of the general developed model in EMTP.

Table 3
Electrical parameters for different grounding grid-units for a typical grid given in Fig. 4.

For grounding grid-units = 10 × 10 = 100 unit				
Grounding grid-unit	R (Ω)	L (μH)	C (μF)	M (μH)
1 (no rods)	6.2810	69.9	2	3
2 (one rod)	6.095	75.8	2.06	4.2
3 (two rods)	5.938	81.7	3.38	5.6
4 (three rods)	5.7944	93.6	3.52	6.7

$$R_g = \frac{\rho}{\pi l}\left(\ln\left(\frac{2l}{\sqrt{2ad}}\right) - 1\right) \tag{9}$$

$$R_g = \frac{\rho}{2\pi l}\left(\ln\left(\frac{4l}{a}\right) - 1\right) \tag{10}$$

where:

l: is the electrode length, d is the burial depth, R is the grounding electrode resistance at low frequency. ρ: is the soil resistivity, a is the electrode radius, I_m is the maximum current and E_c is the soil critical field

The value of the R_{arc} can be evaluated by the model presented in the previous study [32]. The value of the C_g can be calculated as mentioned in the previous study [33]. The values of the different soil resistances and capacitances can be determined as the following:

$$R_{1i\,soil}(t) = R(a + x(t)) - R_g \tag{11}$$

$$C_{1i}(t) = \frac{\rho \in}{R_{1i\,soil}(t)} \tag{12}$$

$$C_g = \frac{\rho \in}{R_g} \tag{13}$$

where R(a + x(t)) is the grounding electrode resistance obtained by adding the ionization length x(t) to the conductor radius a, as given in Eqs. 9 and 10.

The arc conductivity of each TLC can be presented by considering the heat balance $P_b(t)$. $P_b(t)$ is the difference between the instantaneous heat power produced in the arc channel $P_p(t)$ and the instantaneous heat power absorbed by the soil $P_a(t)$. With using the energy balance, P_a can be evaluated in terms of the arc conductivity using Eqs. 14–17.

$$P_b(t) = P_p(t) - P_a(t) \tag{14}$$

$$P_p(t) = v(t)i(t) \tag{15}$$

where $v(t)$ in (V) is the arc voltage and $i(t)$ in (A) is the arc current.

$$P_a = \frac{I_{max}^2}{\sigma_{arc-max}} \tag{16}$$

$$\sigma_{arc-max} = \frac{I_{max}}{V_{max}} \tag{17}$$

With Eqs. 16 and 17, the absorbed heat power Pa can be obtained. Consequently, the arc conductance and its reciprocal (Arc resistance) can be finally obtained. Table 2 presents the main parameters and its values used for developing the TLCs model.

2.3. Electrode lumped equivalent circuit

The proposed soil ionization model by using the TLCs is applied to develop the grounding electrode equivalent circuits with multi-cells of TLCs units. The basic electrical equivalent circuit of each electrode under lightning surge is shown in Fig. 2. Two types of electrodes are considered. The first is the vertical rod with 3 m length and radius 13 mm, while the second is the horizontal electrode that presents the perimeter conductors of the grounding cell. The slow and fast fronted currents are applied to each grounding electrode. The slow-fronted current has 100 kA amplitude and 15.5 kA/μs with time constant (τ = 6.5 μs). The fast-fronted current has 100 kA amplitude with time constant (τ = 1.2 μs). Both currents are simulated based on the International Electrotechnical Commission standard IEC 62,305-3 (Heidler exponential equation for n = 10) [34]. Equivalent electrode resistance and capacitance are computed using Eqs. 18–21 and the influence of the ionization process on the electrode radius is considered by using the effective electrode radius during the ionization in Eqs. 6–11.

$$R_{electrode} = R_g + \sum_{i=1}^{n} \frac{R_{soil\,(i)} * R_{Arc(i)}}{R_{soil\,(i)} + R_{Arc(i)}} \tag{18}$$

The different parameters of the ground electrode with i^{th} can be obtained by using the formula in previous work [35].

$$L_i = \frac{\mu_0 * l_i}{2\pi}\left(\ln\left(\frac{2*l_i}{a}\right) - 1\right) \tag{19}$$

$$R_i = \frac{\rho}{2\pi l_i}\left[\frac{2h + a}{l_i} + \ln\left(\frac{l_i + \sqrt{l_i^2 + a^2}}{a}\right) - \sqrt{1 + \left(\frac{a}{l_i}\right)^2} + \ln\left(\frac{l_i + \sqrt{l_i^2 + 4h^2}}{2h}\right) - \sqrt{1 + \left(\frac{2h}{l_i}\right)^2}\right] \tag{20}$$

$$C_i = \frac{2\pi\varepsilon l_i}{\frac{a_i}{l_i} + \ln\left(\frac{l_i + \sqrt{l_i^2 + a_i^2}}{a_i}\right) - \sqrt{1 + \left(\frac{a_i}{l_i}\right)^2}} \tag{21}$$

where ρ is the soil resistivity and h is the burial depth of the grounding electrode. C_i is the shunt capacitance of the ith segment with a length l_i of and a_i is an ionization zone radius.

2.4. Grounding grid unit-cells

In order to model the whole grounding grid area with and without grounding rods, four grounding grid-units are modelled. The areas of the grounding grid-units are varied from 5 m × 5 m to 40 m × 40 m. The proposed model of the four-grounding grid-units are presented in Fig. 3. The higher the grounding grid-unit area, the lower the ground resistance. In addition, as area of the grounding grid-unit exceeds a certain value, the influence of its dimension on the grounding resistance becomes very low. The first grounding grid-unit consists of horizontal electrode conductor shaped as a rectangle (X(m) × Y(m)) with 0.01 m radius buried in 1 m depth of soil with resistivity of 100 Ω m and relative permittivity of ε_r = 10 (without rods). The configurations of the other three grounding grid-units are the same as the first unit with adding ground-rods in the unit corners. These four-grounding grid-units are used to model typical grounding grid of Cairo-west high voltage substation of 500/220 kV. This substation has four ingoing 500 kV power lines, six outgoing 220 kV power lines and the whole area of the grounding grid is 300 m × 400 m as presented in Fig. 4 (A). All phase conductors of both ingoing and outgoing lines are connected to the ground grid through surge arrestors. The number of grounding unit-cells ranges from 4 units to 100 units to cover the whole area of the substation grounding grid while the unit dimension ranges from (30 m × 40 m) to (5 m × 5 m), respectively. Fig. 4 (B) presents the grounding grid with 100 grounding grid-unit cells. The effects of the number and different areas of each grounding grid-unit will be investigated in the results section.

Each grounding grid unit is simulated by lumped equivalent circuit with the parameters presented in Fig. 5. The grounding grid is presented as network of T connected sections to simulate the different types of the grounding grid units over the whole grounding grid area as shown in Fig. 5. Adding the grounding rods to the grounding grid-units will increase the effective length and area of the grounding grid-unit as

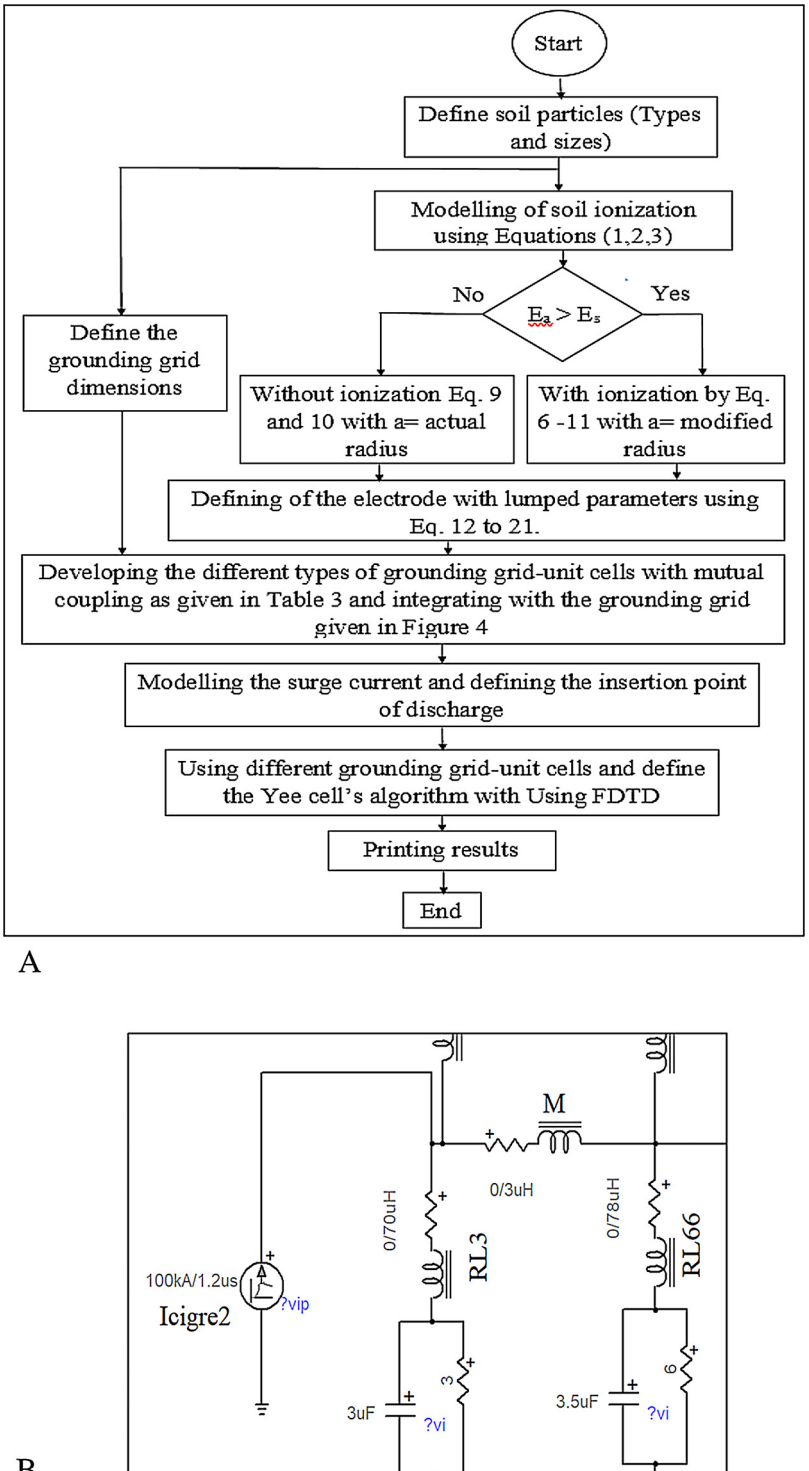

Fig. 7. Flowchart of the steps for the proposed simulation model with and without ionization and a part of EMTP screenshot.

presented in Eqs. 22 and 23.

For the mutual coupling between the different grounding grid-units, the mutual coupling is calculated based on the different prospective arrangements for the conductors over the grounding grid as shown in Fig. 6. The mutual coupling between the grounding grid-units can be calculated by Eq. (24) [33].

$$R_g = \rho\left[\frac{1}{l_T} + \frac{1}{\sqrt{20A}}\left[1 + \frac{1}{1 + h\sqrt{\frac{20}{A}}}\right]\right] \quad (22)$$

where: l_T : is the total conductor length of the grounding unit-cell, A is the area of the grounding unit-cell and h is the burial depth.

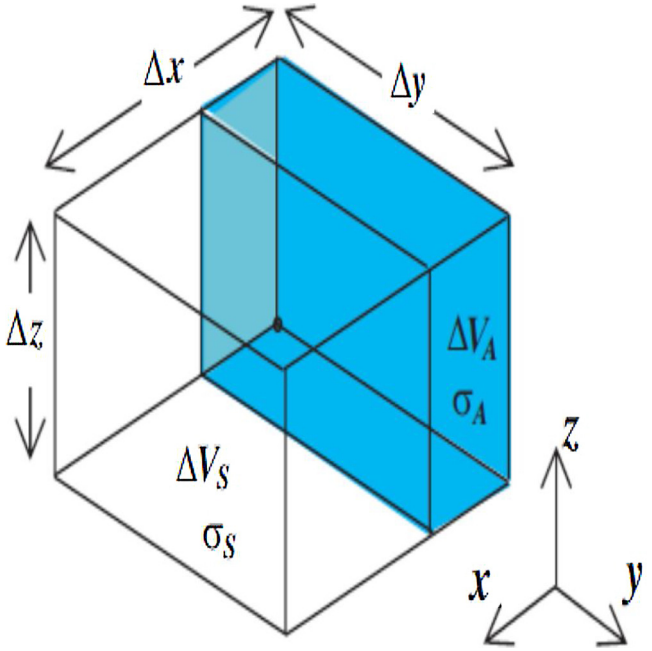

Fig. 8. Elemental cell of the soil grains for Yee's algorithm.

$$l_T = \begin{cases} \sum \text{Conductor length } n = 0 \\ \sum \text{conductor length} + n^{*}\text{Rod length } n > 0 \end{cases} \quad (23)$$

where n is the number of ground rod per each grounding grid-unit.

The mutual coupling among any two grid-units with paralleling conductors can be precisely calculated as the mutual inductance (M) by the following formula [36].

$$M = \frac{\mu_0}{4\pi}\left[\alpha\, ln(\alpha + \sqrt{a^2+h^2}) - \beta\, ln(\beta + \sqrt{\beta^2+h^2}) - \gamma\, ln(\gamma + \sqrt{\gamma^2+h^2}) + \delta\, ln(\delta + \sqrt{\delta^2+h^2}) - \sqrt{\alpha^2+h^2} + \sqrt{\beta^2+h^2} + \sqrt{\gamma^2+h^2} - \sqrt{\delta^2+h^2}\right] \quad (24)$$

where α = a + b + d, β = a + d, γ = b + d and δ = d, respectively.

The electrical parameters of each grounding grid-unit for a typical grid of 100 units for grid area of 400 × 300 m^2 and with grounding resistivity of 100 Ωm are tabulated in Table 3. The methodology tackled for modelling is presented as a flowchart as given in Fig. 7 (A). Meanwhile, Fig. 7 (B) shows a screenshot of a part of the general developed system for electrode presentation with different parameters as given in Table 3. EMTP-RV is used to simulate the system model integrated with Matlab software package by developing multi-scripts to compute the different transient response for the grounding system.

2.5. Field calculation using FDTD

The FDTD formulation of an EM field problem is a convenient scheme to numerically solve scattering problems by using Maxwell's curl equations, together with the constitutive relations of the medium. In order to calculate the transient electromagnetic (EM) over the grounding grid-unit during lightning conditions, the surrounding soil is segmented into very small boxes to shape the elementary cells. The EM field in the elementary cell can be discretized within the curl Maxwell's equations by using Yee's scheme [37,38] as given below:

$$curl\vec{E}(\vec{r}, t) = -\mu(\vec{r}, t)\frac{\partial \vec{H}(\vec{r}, t)}{\partial t} \quad (25)$$

$$curl\vec{H}(\vec{r}, t) = \in(\vec{r}, t)\frac{\partial \vec{E}(\vec{r}, t)}{\partial t} + \sigma(\vec{r}, t)\vec{E}(\vec{r}, t) \quad (26)$$

where $\vec{E}(\bar{r}, t)$ is the electric field vector, $\vec{H}(\bar{r}, t)$ is the magnetic field vector, $\in(\bar{r}, t)$ is the electric permittivity, $\mu(\bar{r}, t)$ is the magnetic permeability, $\sigma(\bar{r}, t)$ is the conductivity of the medium, $\vec{r}$ is the space vector and t is the time.

In cartesian coordinates, the previous equations can be reformatted as the following:

$$\frac{\partial H_x}{\partial t} = \frac{1}{\mu}\left(\frac{\partial E_y}{\partial z} - \frac{\partial E_z}{\partial y}\right), \quad \frac{\partial H_y}{\partial t} = \frac{1}{\mu}\left(\frac{\partial E_z}{\partial x} - \frac{\partial E_x}{\partial z}\right), \quad \frac{\partial H_z}{\partial t} = \frac{1}{\mu}\left(\frac{\partial E_x}{\partial y} - \frac{\partial E_y}{\partial x}\right) \quad (27)$$

$$\frac{\partial E_x}{\partial t} = \frac{1}{\in}\left(\frac{\partial H_z}{\partial y} - \frac{\partial H_y}{\partial z} - \sigma E_x\right), \quad \frac{\partial E_y}{\partial t} = \frac{1}{\in}\left(\frac{\partial H_x}{\partial z} - \frac{\partial H_z}{\partial x} - \sigma E_y\right) \text{ and } \frac{\partial E_z}{\partial t} = \frac{1}{\in}\left(\frac{\partial H_y}{\partial x} - \frac{\partial H_x}{\partial y} - \sigma E_z\right) \quad (28)$$

$$E_t = \sqrt{E_x + E_y + E_z}, \quad H_t = \sqrt{H_x + H_y + H_z} \quad (29)$$

As well, following the Yee's algorithm, the electric and magnetic

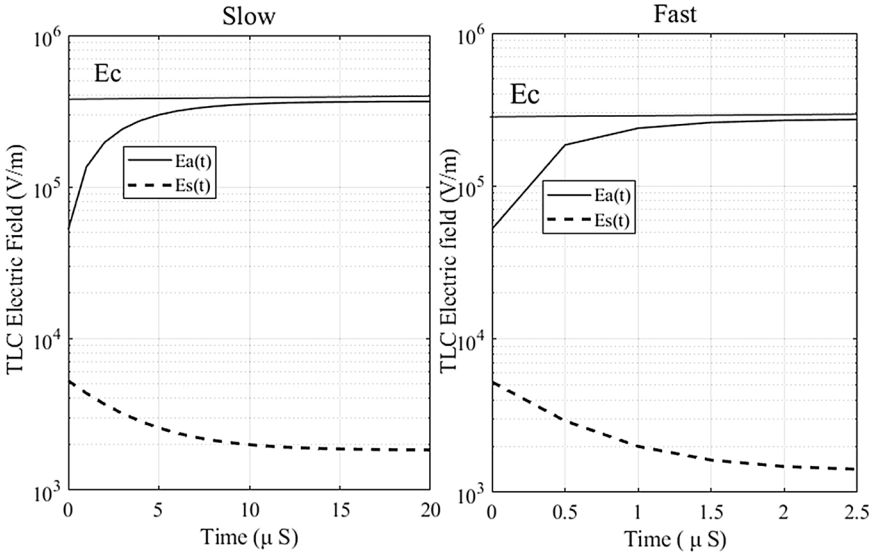

Fig. 9. Electric fields variations with slow and fast fronted in soil particle and air inside the developed two-layer capacitor (TLC). (Y axis is in log scale).

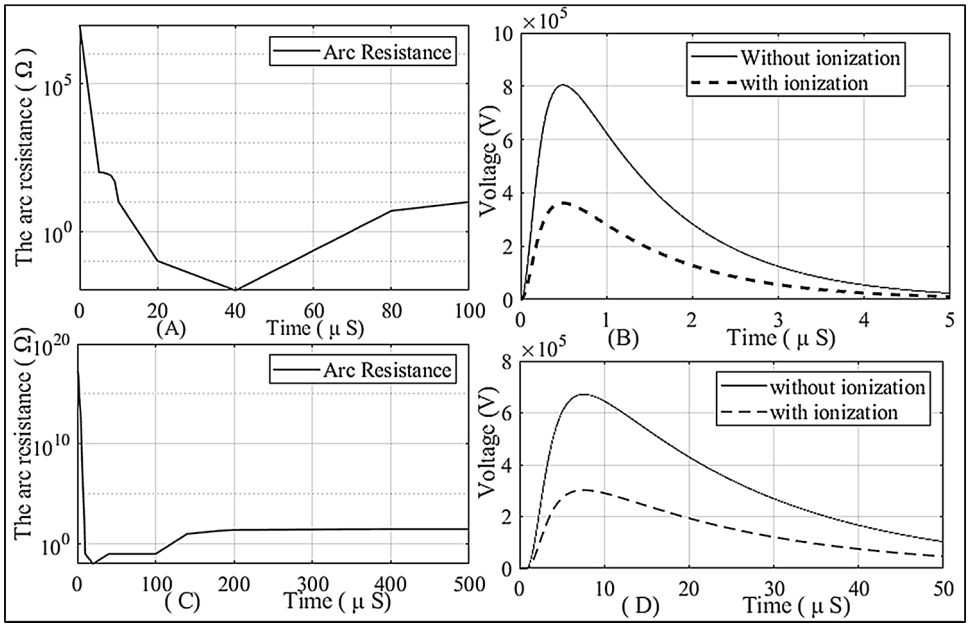

Fig. 10. The Arc resistance and the voltage across the TLC with and without ionization process during slow and fast fronted surges.

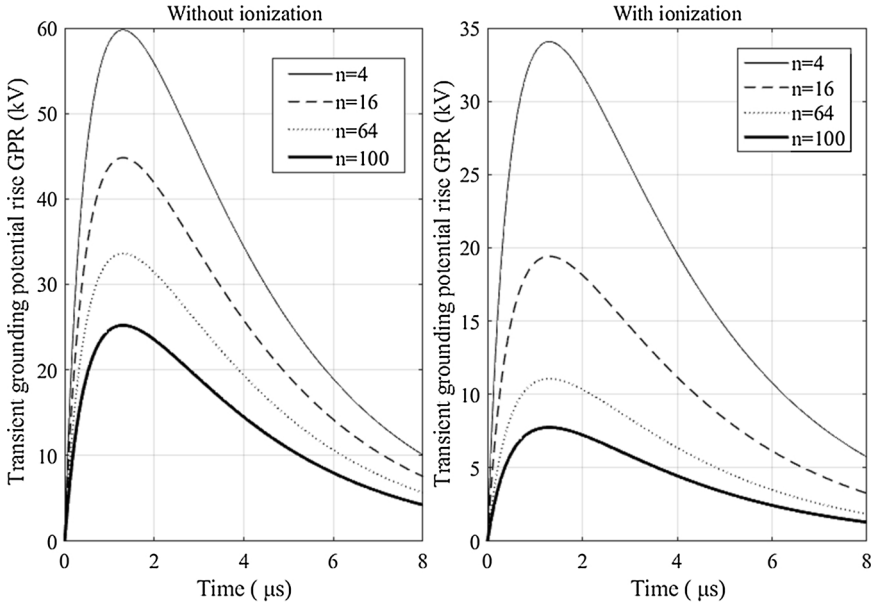

Fig. 11. The transient GPR across the ground grid for different number of the grounding grid-units with and without ionization process.

fields are updated in time at alternate half time steps. First the electric field is computed and then the magnetic one is as well at each time step ΔT. Fig. 8 presents the elemental cell. Soil grains and air voids have different volumes and different conductivities. (A for air; S for soil).

The soil conductivity is considered time varying by assuming the following hypotheses. Inside each elementary cell of the FDTD grid, it is possible to separate the material substances forming the soil from air voids as shown in Fig. 1. In order to use the FDTD scheme precisely for EM surge analysis, some particular features must be introduced. As the finite difference approximation for space and time derivatives are second order, the computational algorithm of the FDTD requires that the spatial increment must be very small compared to the minimum dimension of the scattered object. Therefore, the time step ΔT must satisfy the so-called Courant stability condition [18]. In order to avoid numerical instability in the FDTD algorithm, the sampling time ΔT is given by Eq. 30.

$$\Delta T = \frac{1}{\left(u_{\max}\sqrt{\left(\frac{1}{\Delta x^2}+\frac{1}{\Delta y^2}+\frac{1}{\Delta z^2}\right)}\right)} \tag{30}$$

Δwhere $u_{\max}$:- is the maximum wave phase velocity within the model, Δx, Δy and Δz are the dimension of the small box to form the scattered.

3. Simulation results and discussions

When lightning surges strike the phases or grounding conductors of the power transmission line, a lightning surge current invades the substation. This surge current should be diverted into the grounding grid with the help of the surge arrestors. The lightning surge current is considered to be in order of a 1.2/50 μs for fast surges and of 6.5/300 μs for slow surges with double-exponential wave shape of 100 kA amplitude. The transient performance of the grounding grid-unit with TLCs model and under the lightning surge conditions will be investigated.

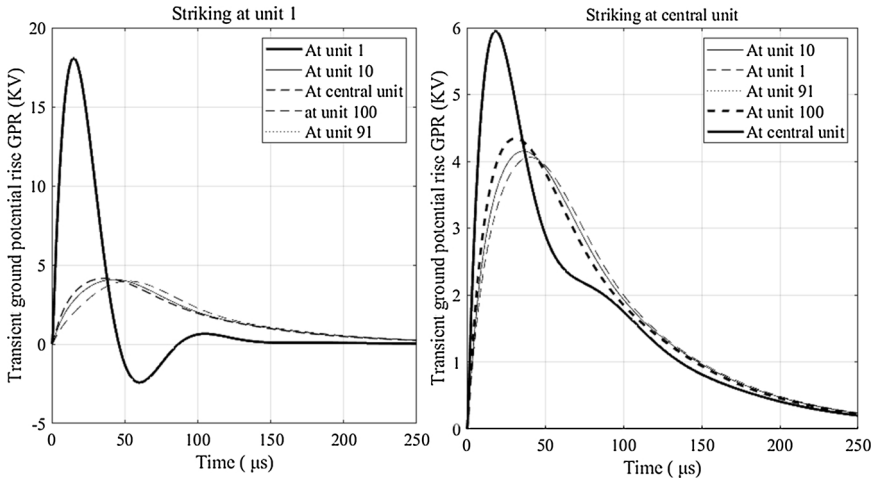

Fig. 12. The transient GPR at different units for striking at one grid corner and the central point of the substation.

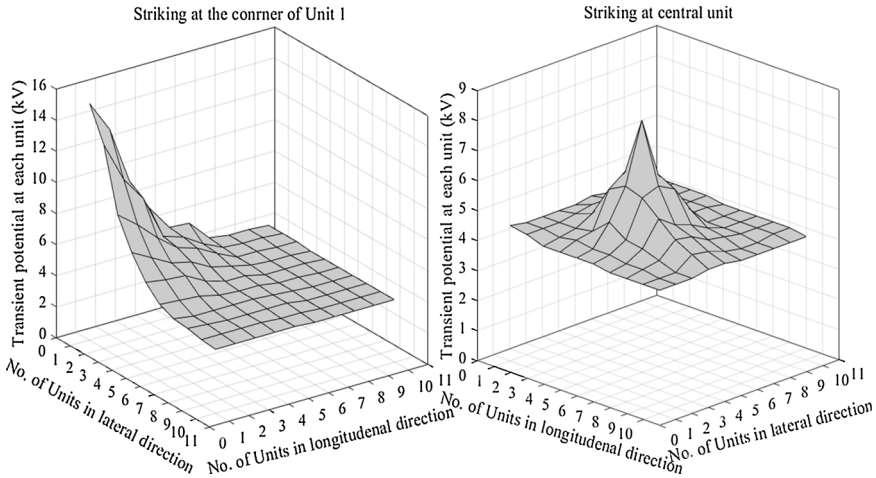

Fig. 13. The transient potential at each unit of the typical grounding grid for striking at Unit 1 and central unit of the substation shown in Fig. 4.

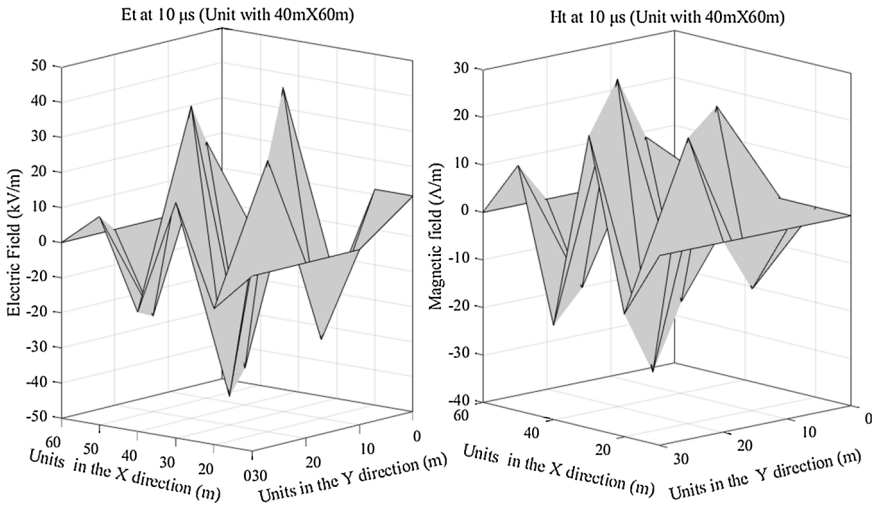

Fig. 14. The transient electric and magnetic fields over one unit of 40 m × 60 m with striking at its central point with 100 kA. (A) Validation of the Grid and TLC Voltages with previous study [30]. (B) Experimental results [40]. (C) Simulation results of proposed model.

The developed model will be validating with previous tackled techniques. Finally, the transient electromagnetic fields will be calculated over the grounding grid-unit by using FDTD.

3.1. TLCs transient performance

With the proposed parameters presented in Table 2 of the TLCs developed model, the transient performance of the TLCs is investigated for fast and slow surges. Fig. 9 presents the electric field variations for

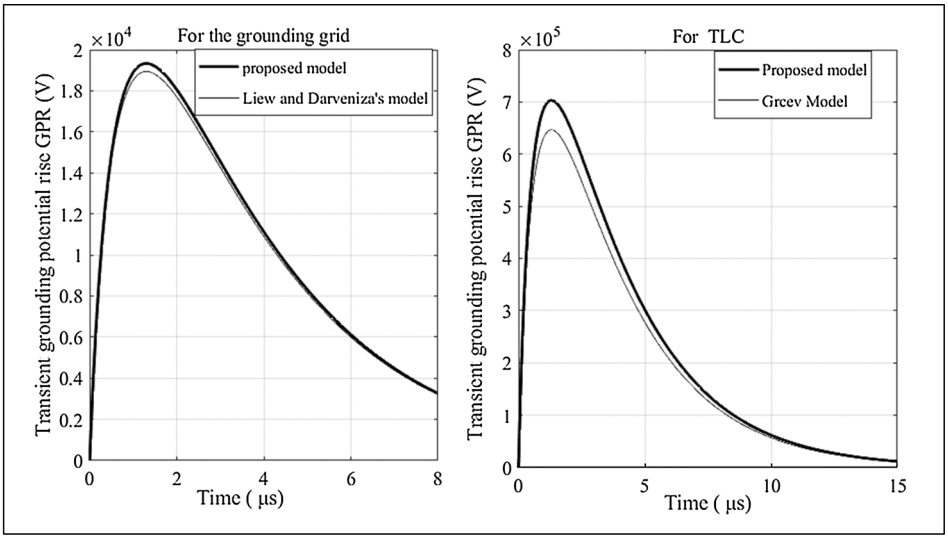

(A) Validation of the Grid and TLC Voltages with previous study [30].

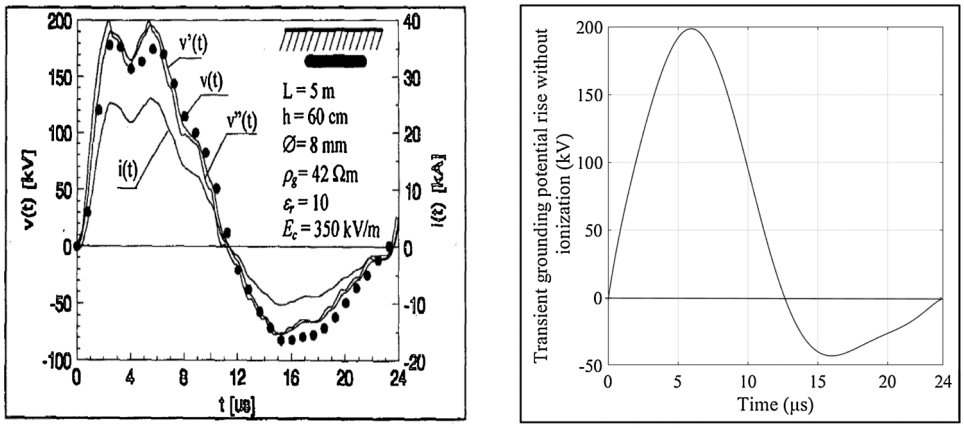

(B) Experimental results [40]. (C) Simulation results of proposed model

Fig. 15. Validation of the one developed grounding unit – cell with the experimental results obtained at [40]. (B) Is the experimental results and (C) simulation results.

the TLC (Air voids and soil particles) for slow and fast front-time surge of 6.5 μs and 1.2 μs, respectively. It can be noted that, the critical field value E_c is about 370 kV/m and 300 kV/m for slow and fast surge current, respectively. Fig. 10 (A,C) presents TLC's Arc resistance variations for fast and slow front-time surges. TLC's Arc resistance drops very fast from very high value during the ionization process (from about 0.5 MΩ to about 20 Ω) within 40 μs and within 200 μs for fast and slow surge, respectively. Fig. 10 (B,D) presents the transient voltage variation of TLC with fast and slow surges. Moreover, the effect of the ionization process is presented. The TLC's maximum voltage of fast surge varies from about 0.8 MV to about 0.4 MV because of ionization process. Meanwhile, for slow surge current, it varies from 0.65 MV to 0.35 MV because of ionization process.

3.2. Effects of the number of the Grounding Grid-Units

The effects of numbers of the grounding grid-units are investigated with consideration of 100 Ω m soil resistivity and with 300 m × 400 m as the whole area of the grounding grid. The numbers of the grid units span a wide range from n = 4 to n = 100 to cover the whole grid area of the typical high voltage substation with 300 m × 400 m. The influences of the numbers of the grounding grid-units under lightning condition of 100 kA striking at one corner of the grid on the grounding potential rise (GPR) with and without ionization process are presented in Fig. 11. All units are without rods. The higher the number of units, the lower the GPR values. For 4 grounding grid-units, the maximum GPR is about 60 kV without ionization, meanwhile it is 33 kV with ionization process. For 100 grounding grid-units, the maximum GPR is about 25 kV without ionization, meanwhile it is about 8 kV with ionization process.

3.3. Effects of lightning striking point

Fig. 12 shows the transient GPR over units at the four corners and the central unit of the substation for lightning strikes of 100 kA at unit 1 and at the central unit, respectively. It can be noted that, the transient GPR is about 18 kV when striking at corner of unit 1 of the grid, but it reaches about 6 kV when striking at the central point of the typical substation shown in Fig. 4. Fig. 13 presents the mesh curve of the maximum values of the transient potential voltage of each unit of the typical grounding grid presented in Fig. 4 for striking point at unit 1 and at the central unit of the substation with ionization process.

3.4. Electromagnetic fields over the grounding grid unit

To evaluate the electromagnetic fields, a grounding grid-unit with

40 m × 60 m is simulated using FDTD techniques. The lightning is simulated with 100 kA and it strikes at the grounding grid-unit center. The electric and magnetic fields are depicted at a time of 10 μs. Fig. 14 presents the total electric and magnetic fields over the simulated grounding grid-unit. The maximum electric field is about 40 kV/m while the maximum magnetic field is about 25 A/m at time of 10 μs over the simulated grounding grid-unit.

3.5. Validation of the developed model

The transient grounding potential rise (GPR) of the TLC proposed model is verified by comparing the voltage responses with the well--known results of simulated model obtained in "Grcev model" found in the literature as shown in the Fig. 15 (A) with title" For TLC". For further validation, the maximum voltage response of the proposed model for the developed grounding grid -unit cell with no rods is compared with the simulated voltage responses of the horizontal electrode system obtained by "Liew and Darveniza model" [30] as shown in Fig. 15 (A) with title "For the grounding grid". Moreover, for comparing with experimental results, a grounding system is developed using the EMTP-RV with implementing soil ionization effect to be consistent with the experimental study shown in Ref. [40] given in Fig. 15 (B). The developed grounding system model is a horizontal conductor of length 5 m and conductor diameter of 8 mm buried underground of 0.6 m considering the soil resistivity of 42 Ω m without ionization and with Ec = 350 kV/m. The surge current is 130 kA. Fig. 15 (B) presents the measured and the computed ground potential rise for horizontal wire tested in Ref. [41]. The i(t) is the impulse injected current, v(t) is the measured ground potential rise, v'(t) is the computed potential rise as proposed in Ref. [41] and v"(t) is the computed ground potential rise by the generalized model proposed in Ref. [39,40]. The transient potential grounding rise (GPR) of the simulated model is presented in Fig. 15 (C). The different parameters of this grounding electrode are calculated using Equations 1920 and 21 as given in Table 3.

4. Conclusions

The Two Layer capacitors (TLC) is implemented to develop simulation model of the soil particles and the surrounding air voids. The TLC model is used as a base model to develop the equivalent electrical parameters of the grounding horizontal and vertical electrodes with and without soil ionization. The proposed model is extended to develop different grounding unit-cells to simulate a typical high voltage substation of 500/220 kV rather than most of other techniques in literature that used some simple electrodes. Moreover, the soil ionization effects are impressively investigated with considering many different design parameters of the grounding systems. The proposed model is quite simple and reduces the complexity of the calculation codes used to develop similar software packages. The transient grounding potential rise (GPR) is calculated during lightning surges by TLCs modelling with and without ionization effects in the time domain using FDTD. The critical electrical field (E_c) of the simulated TLC is about 370 kV/m and 300 kV/m for slow and fast surge current, respectively. The transient voltage of the simulated TLC under fast surges is higher its value under slow surges by about 25%. For the simulated grounding system model with considering the soil ionization, there is a reduction of between 40% and 45% in the value of the transient GPR. This percentage could be subjected to a small deviation. Mainly, this deviation depends on the ground conductivity and the grounding systems. The higher the grounding unit-cells area, the lower the grounding resistance. Moreover, FDTD scheme is implemented to evaluate electromagnetic fields over the grounding unit-cells during the lightning surges. For the simulated model, the maximum electric field over the ground grid is about 40 kV/m meanwhile, the maximum magnetic field is about 25 A/m at time of 10 μs. Finally, the validation of the developed model is performed by comparing with similar work found in literature and it shows high consistency level and good performance of the voltage response.

References

[1] L. Grcev, Modeling of grounding electrodes under lightning currents, IEEE Trans. Electromagn. Compat. 51 (August (3)) (2009) 559–571.
[2] Antonio Carlos Siqueira de Lima, Carlos Portela, Inclusion of frequency-dependent soil parameters in transmission-line modeling, IEEE Trans. Power Del. 22 (January (1)) (2007).
[3] R. Xiong, B. Chen, J.J. Han, Y.Y. Qiu, W. Yang, Q. Ning, Transient resistance analysis of large grounding systems using the FDTD method, Prog. Electromagn. Res. 132 (2012) 159–175.
[4] C.M. Seixas, S. Kurokawa, Member, IEEEA grounding system model directly in time-domain, IEEE Lat. Am. Trans. 14 (October (10)) (2016).
[5] IEEE Guide for Safety in AC substation grounding, IEEE Std. 80–2013, Revision of IEEE Std. 80-2000.
[6] J. He, et al., Optimal design of grounding system considering the influence of seasonal frozen soil layer, IEEE Trans. Power Deliv. 20 (January (l)) (2005) 107–155.
[7] A. Phayomhom, S. Sirisumrannukul, T. Kasirawat, A. Puttarach, Safety design planning of ground grid for outdoor substations in MEA's power distribution system, ECTI Trans. Electrical Eng., Electronics, Commun. 9 (February (1)) (2011) 102–112.
[8] J. Li, et al., Numerical and experimental investigation of grounding electrode impulse-current dispersal regularity considering the transient ionization phenomenon, IEEE Trans. Power Del. 26 (October (4)) (2011) 2647–2658.
[9] B. Zhang, et al., Numerical analysis of transient performance of grounding systems considering soil ionization by coupling moment method with circuit theory, IEEE Trans. Magn. 41 (May (5)) (2005) 1440–1443.
[10] B. Zhang, et al., Effect of grounding system on electromagnetic fields around building struck by lightning, IEEE Trans. Magn. 46 (August (8)) (2010) 2955–2958.
[11] A. Elzowawi, et al. Investigation of soil ionization propagation in two- layer soil samples 978-1-4673-9682-0/15/$31.00 ©2015 IEEE.
[12] M. Tsumura, Y. Baba, N. Nagaoka, A. Ametani, FDTD simulation of a horizontal grounding electrode and modeling of its equivalent circuit, IEEE Trans Electromagn. Compat. 48 (November (4)) (2006) 817–825.
[13] Masanobu Tsumura, Yoshihiro Baba, Naoto Nagaoka, Akihiro Ametani, FDTD simulation of a horizontal grounding electrode and modeling of its equivalent circuit, IEEE Trans. Electromagn. Compat. 48 (November(4)) (2006) 817–825.
[14] Masanobu Tsumura, Yoshihiro Baba, Naoto Nagaoka, Akihiro Ametani, FDTD simulation of a horizontal grounding electrode and modeling of its equivalent circuit, IEEE Trans. Electromagn. Compat. 48 (November (4)) (2006) 817–825.
[15] Run Xiong, Bin Chen, Cheng Gao, Yun Yi, Wen Yang, FDTD calculation model for the transient analyses of grounding systems, IEEE Trans. Electromagn. Compat. 56 (October (5)) (2014).
[16] A.C. Liew, M. Darveniza, Dynamics model of impulse characteristics of concentrated earth, Proc. IEE 121 (February (2)) (1974) 123–135.
[17] G. Ala, P.L. Buccheri, P. Romano, F. Viola, Finite difference time domain simulation of earth electrodes soil ionization under lightning surge condition, IET Sci., Meas. Technol. 2 (May (3)) (2008) 134–145.
[18] Y. Liu, N. Theethayi, R. Thottappillil, R.M. Gonzales, M. Zitnik, An improved model for soil ionization around grounding system and its application to stratified soil, J. Electrostatics 60 (March (2–4)) (2004) 203–209.
[19] S. Sekioka, M.I. Lorentzou, M.P. Philippakou, J.M. Prousalidis, Current dependent grounding resistance model based on energy balance of soil ionization, IEEE Trans. Power Deliv. 21 (January (1)) (2006) 194–201.
[20] R.E. Leadon, T.M. Flanagen, C.E. Mallon, R. Denson, Effect of ambient gas on ARC initiation characteristics in soil, IEEE Trans. Plasma Sci. IEEE Nucl. Plasma Sci. Soc. 30 (November (6)) (1983) 4572–4576.
[21] A.M. Mousa, The soil ionization gradient associated with discharge of high currents into concentrated electrodes, IEEE Prog. Electromagnetics Res. B 14 (2009).
[22] Thaís L.Tdos Santos, et al., Soil ionization in different types of grounding grids simulated by FDTD method, 2009 SBMO/IEEE MTT-S International Microwave and Optoelectronics Conference (IMOC), (2009), pp. 127–132.
[23] G. Ala, M.L.D. Silvestre, F. Viola, Soil ionization due to high pulse transient currents leaked by earth electrodes, Prog. Electromagn. Res. B 14 (2009) 1–21.
[24] J. He, R. Zeng, B. Zhang, Methodology and Technology for Power System Grounding, 1st ed., John Wiley & Sons, Singapore, 2013.
[25] A.C. Liew, M. Darveniza, Dynamics model of impulse characteristics of concentrated earth, Proc. IEE 121 (February (2)) (1974) 123–135.
[26] P.L. Bellaschi, R.E. Armington, A.E. Snowden, Impulse and 60-cycle characteristics of driven grounds–II, Trans. Am. Inst. Electr. Eng. 61 (6) (1942) 349–363.
[27] Mehrdad Mokhtari, Zulkurnain Abdul–Malek, Gevork B. Gharehpetian, A New Soil Ionization Model for Grounding Electrodes, Wiley, 2016, https://doi.org/10.1002/etep.2266.
[28] M.J. Dumbleton, The British Soil Classification System for Engineering Purposes: its Development and Relation to Other Comparable Systems, Report 1030. Transport and Road Research Laboratory Environment: Crowthorne, Berkshire, 1981.
[29] IEEE recommended practice for grounding of industrial and commercial power systems. IEEE Std 142–2007 (Revision of IEEE Std 142–1991). 2007:1–225.
[30] A.C. Liew, M. Darveniza, Dynamic model of impulse characteristics of concentrated earths, Proc. Inst. Electr. Eng. 121 (2) (1974) 123–135.
[31] M. Mokhtari, Z. Abdul–Malek, Z. Salam, An improved circuit-based model of a

grounding electrode by considering the current rate of rise and soil ionization factors, IEEE Trans. Power Deliv. 30 (1) (2015) 211–219.
[32] G. Ala, P.L. Buccheri, P. Romano, F. Viola, Finite difference time domain simulation of earth electrodes soil ionization under lightning surge condition, IET Sci. Meas. Technol. 2 (May (3)) (2008) 134–145.
[33] E.D. Sunde, Earth Conduction Effects in Transmission Systems, 2nd ed., Dover, New York, 1968.
[34] Ed.1: Protection Against Lightning—Part 3: Physical Damage to Structures and Life Hazard, IEC 62305-3, 2006.
[35] Rong Zeng, et al., Lightning impulse performances of grounding grids for substations considering soil ionization, IEEE Trans. Power Deliv. 23 (April (2)) (2008).
[36] M.M.B. Narayanan, S. Parameswaran, D. Mukhedkar, Transient performance of grounding grids, IEEE Trans. Power Del. 4 (October (4)) (1989) 2053–2059.
[37] A. Taflove, S. Hagness, Computational Electro Dynamics: the Finite-difference Time-domain Method, Artech House, Boston, MA, 2000.
[38] D.M. Sullivan, Electromagnetic simulation using the FDTD method, IEEE Press Ser. RF Microw. Technol. (July) (2000).
[39] L. Grcev, Time- and frequency-dependent lightning surge characteristics of grounding electrodes, IEEE Trans. Power Deliv. 24 (4) (2009) 2186–2196.
[40] A. Geri, Behaviour of grounding systems excited by high impulse currents: the model and its validation, IEEE Trans. Power Deliv. 14 (3) (1999) 1008–1017.
[41] E. Garbagnati, A. Geri, G. Sartorio, G.M. Veca, Non-Linear Behaviour of ground electrodes under lightning surge currents: computer modelling and comparison with experimental results, IEEE Trans. Magnetics 28 (March (2)) (1992) 1442–1445.